J. Fluid Mech. (2005), *vol.* 533, *pp.* 47–56.
doi:10.1017/S0022112005003897 Printed in the United Kingdom

A linearized kinetic formulation including a second-order slip model for an impulsive start problem at arbitrary Knudsen numbers

By N. G. HADJICONSTANTINOU AND H. A. AL-MOHSSEN

Mechanical Engineering Department, Massachusetts Institute of Technology, 77 Massachusetts Avenue, Room 3-364, Cambridge, MA 02139, USA

(Received 14 August 2004 and in revised form 8 December 2004)

We investigate the time evolution of an impulsive start problem for arbitrary Knudsen numbers (Kn) using a linearized kinetic formulation. The early-time behaviour is described by a solution of the collisionless Boltzmann equation. The same solution can be used to describe the late-time behaviour for $Kn \gg 1$. The late-time behaviour for $Kn < 0.5$ is captured by a newly proposed second-order slip model with no adjustable parameters. All theoretical results are verified by direct Monte Carlo solutions of the nonlinear Boltzmann equation. A measure of the timescale to steady state, normalized by the momentum diffusion timescale, shows that the timescale to steady state is significantly extended by ballistic transport, even at low Knudsen numbers where the latter is only important close to the system walls. This effect is captured for $Kn < 0.5$ by the slip model which predicts the equivalent effective domain size increase (slip length).

1. Introduction

In this paper we investigate the transient behaviour of a monoatomic hard-sphere gas between two infinite flat walls a distance L apart which at $t = 0$ start moving in their plane and in the same direction with velocity U. This investigation is part of an ongoing effort to extend our current understanding of transport beyond the classical Navier–Stokes description which only holds when characteristic lengthscales (L) are significantly longer then the molecular mean free path (λ), or, in other words, when the Knudsen number $Kn = \lambda/L$ is very small.

This impulsive start problem has been extensively studied in the no-slip Navier–Stokes limit in connection with a large number of practical applications; its solution is also of educational value and can be found in a variety of textbooks, e.g. Mills (1992). The extension of this problem to all Kn is relevant to current practical applications (Ho & Tai 1998) in connection with micro- and nanoscale science and engineering; it is also of considerable value as a vehicle for understanding transport in the transition regime ($0.1 \lesssim Kn \lesssim 10$) and evaluating models of it. In this work, the applicability of two such models is evaluated by comparing their predictions to direct Monte Carlo solutions of the nonlinear Boltzmann equation. The first is an analytical solution developed in this paper which is based on the collisionless Boltzmann equation (Sone 1964), and shown to be valid for early times for all Knudsen numbers and late times for large Knudsen numbers. The second model evaluated is a recently proposed (Hadjiconstantinou 2003) second-order slip model for hard-sphere gases which extends

the applicability of the Navier–Stokes† description in one-dimensional problems up to $Kn \approx 0.4$ under linearized conditions ($Re \ll 1$, where Re is the Reynolds number). This paper demonstrates that the key to the development of a successful second-order slip model is the careful interpretation of the flow field in a manner which accounts for deviations from Navier–Stokes behaviour in the near-wall regions known as Knudsen layers (Cercignani 1988). In particular, as the Knudsen number increases beyond 0.1, these regions extend over a non-negligible part of the flow; this has caused previous approaches (to second-order slip) that attempt to fit the velocity profile thoroughout the physical domain to fail. On the other hand, properly accounting for the Knudsen layers leads to a predictive model (Hadjiconstantinou 2003) with no adjustable parameters which is in agreement with solutions of the Boltzmann equation (Hadjiconstantinou 2005) and, as discussed below, experimental data.

In our computations we used the hard-sphere model for computational convenience but also to facilitate comparison with the hard-sphere slip model that was recently developed. The hard-sphere model has been shown to provide reasonable descriptions of isothermal gas flows. In the next section we show that under the linearized conditions assumed in our investigation the flow studied here is isothermal. Second-order slip models for even more realistic gas models can be subsequently developed using the approach outlined in Hadjiconstantinou (2003).

2. Problem description

We consider a dilute gas of kinematic viscosity ν between two infinitely long, smooth and fully accommodating (diffusely reflecting) walls in the (x, z)-plane, placed at $y = -L/2$ and $y = L/2$ respectively. At time $t = 0$ both walls start to move in the x-direction with velocity U. The gas temperature and density, which as shown below remain constant in time and uniform in space, will be denoted by T and ρ, respectively. The fluid velocity in the axial direction is denoted $u = u(y)$.

Our solution assumes that U is small enough so that the governing kinetic equation (and boundary conditions) can be linearized. This requirement can be expressed in kinetic terms as

$$U/c_m = \sqrt{\bar{\gamma}/2}M \ll 1 \tag{2.1}$$

that is, the Mach number (M) is small. Here, $c_m = \sqrt{2kT/m}$ is the most probable molecular speed, $\bar{\gamma}$ is the ratio of specific heats, k is Boltzmann's constant, and m is the molecular mass. In this limit, as shown below, the velocity and temperature fields are decoupled, and the isothermal approximation is reasonable.

An implication of the linearization condition (2.1) stems from the relation

$$M \approx Re\, Kn \tag{2.2}$$

where $Re = UL/\nu$ is the Reynolds number. Relation (2.2) implies that any formulation based on the assumption $M \ll 1$ is limited to $Re \ll 1$ for $Kn > 0.1$. Although convection is not important in the problem studied here, this discussion aims to clarify that, when referring to second-order slip models and the associated extension of the Navier–Stokes description to $Kn > 0.1$ the condition $Re \ll 1$ is implied, because, as discussed in § 4.2, the second-order slip model used here is based on such an assumption ($M \ll 1$).

† The term Navier–Stokes is used here to denote the continuum hydrodynamic description with diffusive transport (viscous, Fourier, Fickian) closures appropriate to the $Kn \ll 1$ limit.

2.1. *Boltzmann equation formulation*

Although the nonlinear Boltzmann equation can describe all Knudsen regimes, analytical solutions are very difficult to obtain. In this section we obtain an analytical solution for the collisionless limit.

Let $\boldsymbol{c}=(c_x, c_y, c_z)$ be the molecular velocity vector. By writing the distribution function of molecular velocities as $f=\rho F(1+\phi)$ and neglecting higher-order terms in ϕ, we obtain the linearized collisionless Boltzmann equation (Cercignani 1988)

$$\frac{\partial \phi}{\partial t} + c_y \frac{\partial \phi}{\partial y} = 0. \tag{2.3}$$

Here

$$F = \left(\frac{1}{\pi c_m^2}\right)^{3/2} \exp\left(-\frac{c_x^2 + c_y^2 + c_z^2}{c_m^2}\right) \tag{2.4}$$

is the equilibrium Maxwellian distribution function, and

$$u = \int c_x \phi F \, \mathrm{d}c \tag{2.5}$$

is the macroscopic velocity in the x direction.

In the above we have taken the density and temperature perturbation fields to be zero. This can be seen to be the case later, where the solution for ϕ will be found to be an odd function of c_x (see equations (2.9), (2.10)). Although our solution is limited to the collisionless limit, similar arguments can be made for the whole Kn range, at least in the BGK approximation (Sone 1964). In the Navier–Stokes limit, this is consistent with the Navier–Stokes theory which predicts that the isothermal approximation is reasonable when the Brinkman number $Br=\mu U^2/(\kappa T)$ is small, where μ is the coefficient of viscosity and κ is the thermal conductivity. Using the fact that for a hard-sphere gas $\kappa/\mu \approx 15\,\mathrm{k}/(4\,m)$ we see that $Br \approx mU^2/(15\,kT) = (4\bar{\gamma}/15)M^2 \ll 1$ is automatically satisfied when the linearization condition (2.1) holds.

The fact that ϕ is an odd function of c_x also means that the mass flux to the wall remains equal to its equilibrium value and thus the linearized boundary conditions of the two walls can be written as (Sone 1964)

$$\phi = \frac{2c_x U}{c_m^2} \quad c_y > 0 \ \text{ at } \ y = -\frac{L}{2}, \tag{2.6}$$

$$\phi = \frac{2c_x U}{c_m^2} \quad c_y < 0 \ \text{ at } \ y = \frac{L}{2}. \tag{2.7}$$

The initial condition is $\phi = 0$. Taking the Laplace transform of equation (2.3) we obtain

$$\frac{\partial \hat{\phi}}{\partial y} + \frac{s}{c_y}\hat{\phi} = 0 \tag{2.8}$$

where s is the Laplace variable and $\hat{}$ denotes the Laplace transform of a function. The solution of this equation is given by

$$\hat{\phi} = \frac{2c_x U}{s c_m^2} \exp\left[-\frac{s}{c_y}\left(y + \frac{L}{2}\right)\right], \ c_y > 0, \tag{2.9}$$

$$\hat{\phi} = \frac{2c_x U}{s c_m^2} \exp\left[-\frac{s}{c_y}\left(y - \frac{L}{2}\right)\right], \ c_y < 0. \tag{2.10}$$

The first moment of the solution gives the following equation for the velocity field:

$$\hat{u} = \frac{U}{s\sqrt{\pi}}\left\{ J_0\left[\left(\frac{s}{c_m}\right)\left(\frac{L}{2}+y\right)\right] + J_0\left[\left(\frac{s}{c_m}\right)\left(\frac{L}{2}-y\right)\right]\right\} \tag{2.11}$$

where

$$J_n(\zeta) = \int_0^\infty \xi^n \exp\left[-\left(\xi^2 + \frac{\zeta}{\xi}\right)\right] \mathrm{d}\xi. \tag{2.12}$$

The properties of the functions $J_n(\zeta)$ can be found in Abramowitz & Stegun (1964).

The shear stress τ_{xy} is given by

$$\tau_{xy} = \rho \int (c_x - u) c_y (1+\phi) F \,\mathrm{d}c = \rho \int c_x c_y \phi F \,\mathrm{d}c \tag{2.13}$$

leading to

$$\hat{\tau}_{xy} = \rho \frac{U c_m}{s\sqrt{\pi}}\left[J_1\left(\frac{s(L/2+y)}{c_m}\right) - J_1\left(\frac{s(L/2-y)}{c_m}\right)\right]. \tag{2.14}$$

2.2. *The direct simulation Monte Carlo method*

All of the theoretical results developed in this paper are verified by numerical solutions of the nonlinear Boltzmann equation, obtained using a stochastic molecular simulation technique known as the direct simulation Monte Carlo (DSMC). Consistency between DSMC solutions and solutions of the Boltzmann equation in the limit of infinitesimal discretization and a large number of particles was shown by Wagner (1992). Alexander, Garcia & Alder (1998) have shown that the transport coeffcients exhibit quadratic convergence with the cell size. Hadjiconstantinou (2000) and Garcia & Wagner (2000) have shown the same behaviour for the timestep.

3. Solution for early times

At early times $\varepsilon t \ll 1$, the effect of molecular collisions is small. Here ε is the collision frequency which is related to the mean free path by $\varepsilon = 2c_m/(\sqrt{\pi}\lambda)$. We can thus describe the hydrodynamic fields for short times for arbitrary Kn using equation (2.11). This limit also approximates for all times the physical situation $\varepsilon L/(2c_m) = 1/(\sqrt{\pi}Kn) \to 0$, that is, systems so small that their characteristic timescale $L/(2c_m)$ is much shorter than the collision time. In the next section, where the late-time behaviour of systems is studied, we derive a more quantitative criterion for the characteristic size of such systems.

In the $\varepsilon t \ll 1$ limit

$$\begin{aligned} u &= \frac{U}{\sqrt{\pi}}\left[\int_{\frac{L/2+y}{c_m t}}^\infty \exp(-\xi^2)\mathrm{d}\xi + \int_{\frac{L/2-y}{c_m t}}^\infty \exp(-\xi^2)\,\mathrm{d}\xi\right] \\ &= \frac{U}{2}\left[\mathrm{erfc}\left(\frac{L/2+y}{c_m t}\right) + \mathrm{erfc}\left(\frac{L/2-y}{c_m t}\right)\right] \end{aligned} \tag{3.1}$$

where $\mathrm{erfc}(\zeta) = 1 - (2/\sqrt{\pi})\int_0^\zeta \exp(-\xi^2)\,\mathrm{d}\xi$ is the complementary error function. It is remarkable that this ('non-interacting' limit) solution is similar in form to the semi-infinite body solution of the diffusive (Navier–Stokes) problem; in the latter solution the diffusive lengthscale $\sqrt{\nu t}$ takes the role of the ballistic lengthscale $c_m t$, provided that $\sqrt{\nu t} \ll L/2$ such that the disturbances from the two walls are not 'interacting'.

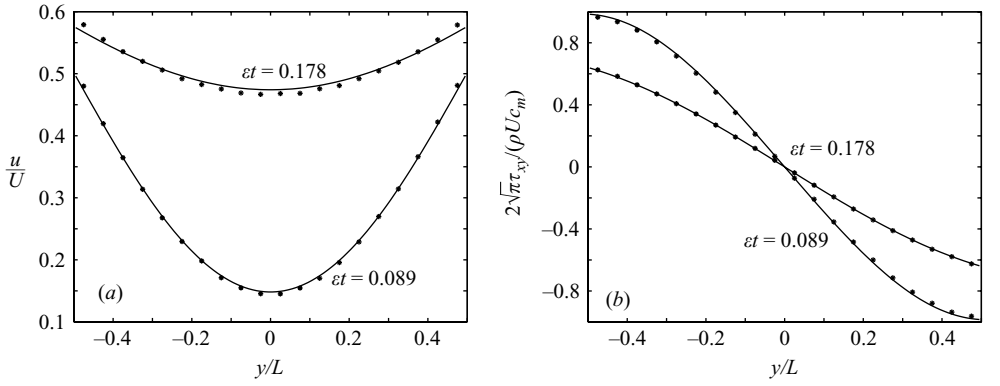

FIGURE 1. Normalized velocity and stress fields at $\varepsilon t = 0.089$ and 0.178 for $Kn = 6.26$. (*a*) Comparison between equation (3.1) and DSMC solutions. (*b*) Comparison between equation (3.2) and DSMC solutions. The DSMC solutions are denoted by stars.

Inverting equation (2.14) back to the time domain we obtain

$$\tau_{xy} = \frac{\rho U c_m}{2\sqrt{\pi}} \left\{ \exp\left[-\left(\frac{L/2 + y}{c_m t} \right)^2 \right] - \exp\left[-\left(\frac{L/2 - y}{c_m t} \right)^2 \right] \right\}. \tag{3.2}$$

Comparison of the above results with DSMC simulations is shown in figure 1. The agreement between the two solutions is excellent at $\varepsilon t = 0.089$ and acceptable at $\varepsilon t = 0.178$, as one would expect. Although these comparisons are for a rather high Knudsen number (= 6.26), as noted above, results (3.1), (3.2) are expected to be valid for all Kn as long as $\varepsilon t \ll 1$.

4. Solution for late times

Although the late-time behaviour for $Kn \ll 1$ coincides with $\varepsilon t \gg 1$, as discussed in the previous section, when the Knudsen number increases beyond $Kn \gtrsim 1$, characteristic late-time behaviour timescales are not necessarily much longer than the collision time $1/\varepsilon$. For this reason, we will consider the two limits, $Kn \gg 1$ and $Kn \ll 1$, separately.

4.1. *The ballistic limit* ($Kn \gg 1$)

As noted in the previous section, equation (3.1) also describes systems in the $Kn \to \infty$ limit for all (relevant) times. At late times ($L/(2c_m t) \ll 1$) we obtain from (3.1)

$$u = U\left(1 - \frac{2}{\sqrt{\pi}} \frac{L}{2c_m t}\right) + O\left(\left(\frac{L}{2c_m t}\right)^3\right), \tag{4.1}$$

that is, the velocity profile is flat. Let us consider t_{90}, the time for the average velocity to reach 90% of U, a characteristic timescale that we will also consider later: according to (4.1), $\varepsilon t_{90} = 20/(\pi Kn)$. For this prediction to be accurate, $\varepsilon t_{90} \ll 1$ also has to hold which implies that equations (3.1), (3.2) and (4.1) will describe the behaviour (up to times of the order of t_{90}) for systems which are characterized by $Kn \gg 20/\pi$. Although an analytical solution taking into account the effect of collisions for, say, $Kn \gtrsim 5$ could be developed using the BGK model of the Boltzmann equation, preliminary results indicate that in the neighbourhood of $Kn \approx 10$ the error introduced by the BGK approximation is comparable to the error obtained by completely neglecting collisions.

4.2. *The diffusive limit: the Navier–Stokes solution*

For $Kn \ll 1$ the gas behaviour is captured by the Navier–Stokes equations. It is well known that the validity of the Navier–Stokes description can be extended to $Kn \simeq 0.1$ by use of 'first-order' slip flow boundary conditions (Cercignani 1988). Due to the significant computational advantage the Navier–Stokes formulation enjoys, second-order slip models which extend the applicability of Navier–Stokes formulations even further are very desirable. However, a number of second-order slip models proposed in the past have not been successful in a predictive sense for reasons that will be discussed below.

Our discussion below demonstrates that it is indeed possible to obtain correct hydrodynamic fields to second order in the Knudsen number using a slip-corrected Navier–Stokes description, provided that deviations from Navier–Stokes in the near-wall regions are correctly accounted for. More specifically, within the asymptotic analysis which leads to the slip-flow description, slip-flow boundary conditions provide *effective boundary conditions for the Navier–Stokes component of the flow field* $\tilde{u}$, while in the near-wall regions a kinetic boundary layer needs to be added in order to capture the complete solution of the Boltzmann equation for the flow field (Cercignani 1964). In other words, $u = \tilde{u} + u_{KN}$ where u_{KN} is the Knudsen layer correction which satisfies $u_{KN} \to 0$ as $(y - y_w)/\lambda \to \infty$, where y_w is the wall location. For engineering purposes, however, the effective thickness of the Knudsen layer can be taken to be approximately 1.5λ (Hadjiconstantinou 2005). Thus, as the Knudsen number increases beyond, say, $Kn \approx 0.1$, the Knudsen layers cover a significant amount of the domain and need to be taken into account. This was put onto a firmer theoretical footing by Cercignani who showed that the contribution of the Knudsen layers is such that the true bulk flow speed $\int_{-L/2}^{L/2} u \, \mathrm{d}y$ differs from the slip flow approximation $\int_{-L/2}^{L/2} \tilde{u} \, \mathrm{d}y$ to $O(Kn^2)$ (Cercignani 1964).

The existence of the Knudsen layers has a number of interesting consequences. First it makes direct comparison between slip-flow results and Boltzmann equation solutions difficult and requires special care when interpreting slip-flow results. It also implies that a successful second-order slip model is one that does not agree with Boltzmann equation solutions within 1.5λ from system walls. This last observation explains why previous attempts to determine the second-order slip coefficient from fitting DSMC flow fields in the complete simulation domain have not been successful.

Here we use a second-order slip model for a hard-sphere gas recently proposed by the author (Hadjiconstantinou 2003). According to this model, for one-dimensional flows, the slip velocity $\tilde{u}|_{\mathrm{wall}} - u_{\mathrm{w}}$ is given by

$$\tilde{u}|_{\mathrm{wall}} - u_{\mathrm{w}} = \alpha\lambda \left.\frac{\partial \tilde{u}}{\partial \eta}\right|_{\mathrm{wall}} - \beta\lambda^2 \left.\frac{\partial^2 \tilde{u}}{\partial \eta^2}\right|_{\mathrm{wall}} \tag{4.2}$$

where $\alpha = 1.11$, $\beta = 0.61$ have been determined by solution of the Boltzmann equation (see Hadjiconstantinou 2005 for discussion). Here, $|_{\mathrm{wall}}$ denotes quantities evaluated at the wall, u_{w} is the wall velocity, and η is the normal to the wall pointing into the gas. Higher-dimensional flows are briefly discussed below. The Boltzmann equation solutions on which this model is based assume a steady flow, flat walls, no gradients in the direction of the flow and linearized ($M \ll 1$, $Re \ll 1$) conditions.

The contribution of the Knudsen layer can be most conveniently accounted for in an average sense, i.e. when calculating averages over the domain. In a one-dimensional

flow field, the mean (bulk) flow velocity is given by

$$u_b = \frac{1}{L}\int_{-L/2}^{L/2} u \, \mathrm{d}y = \frac{1}{L}\int_{-L/2}^{L/2} \left[\tilde{u} + \delta\lambda^2 \frac{\partial^2 \tilde{u}}{\partial y^2}\right] \mathrm{d}y \tag{4.3}$$

where the contribution of the Knudsen layer is captured by the second term in the integral with $\delta = 0.296$ (Hadjiconstantinou 2003).

A direct consequence of the above relation is that in Poiseuille-type flows where the curvature (of the Navier–Stokes component) of velocity is constant, experimental measurement of the flow rate (bulk flow velocity) yields an 'effective' second-order slip coefficient $\beta - \delta$ (Hadjiconstantinou 2005). Recent experiments in helium and nitrogen (Maurer *et al.* 2003) report a second-order slip coefficient of approximately 0.25 ± 0.1 which is in good agreement with the model prediction $\beta - \delta = 0.31$.

Navier–Stokes solutions using the above second-order slip model have been compared to DSMC simulations of pressure-driven flow in two-dimensional channels (Hadjiconstantinou 2003). Very good agreement was found up to $Kn \approx 0.4$; it was also found that the second-order slip flow model remains qualitatively accurate well beyond $Kn = 0.4$. These results demonstrate that this model, even in its one-dimensional form, may be used in higher-dimensional flows which vary slowly in one or more dimensions; examples of such flows include those for which the locally fully developed or long-wavelength approximations are appropriate. Although an augmented form of this slip model suitable for higher-dimensional flows exists, it has not been validated yet (Hadjiconstantinou 2005).

The present work serves as an independent validation of the slip model which provides a comparison for both the flow and stress fields for an unsteady flow – recall that the slip model is based on a steady flow assumption. Our comparison provides evidence that the slip model remains accurate at timescales as short as $5\varepsilon^{-1}$; in other words, flows developing at time scales that are long compared to the molecular collision time are effectively quasi-static in the context of second-order slip.

For the impulsive start problem we solve the governing equation

$$\frac{\partial \tilde{u}}{\partial t} = \nu \frac{\partial^2 \tilde{u}}{\partial y^2} \tag{4.4}$$

subject to the slip boundary condition (4.2) using a finite difference method.

Figures 2 and 3 show a representative comparison between the velocity and stress fields obtained by the Navier–Stokes and DSMC descriptions at $Kn = 0.21$; due to the problem symmetry, only half of the physical domain ($-0.5 \leqslant y/L \leqslant 0$) is shown. Provided that these results are interpreted correctly (by taking into account the existence of the Knudsen layer) the agreement is excellent. At $Kn = 0.21$, each Knudsen layer extends from each wall to cover more than 60% of the physical half-domain; in the half-domain shown here, direct comparison between DSMC results (u) and second-order slip results ($\tilde{u}$) is thus meanignful only in the region $-0.185 \leqslant y/L \leqslant 0$ delimited by the vertical dotted line. As figure 2(a) confirms, the agreement in this region is very good, whereas for $y/L \lesssim -0.185$ the presence of the Knudsen layer is clear. It is also possible to see that in the Knudsen layer, $u - \tilde{u}$ scales with the curvature of $\tilde{u}$, as equation (4.3) suggests. On the other hand, the stress field in figure 2(b) is captured throughout the domain with agreement that can only be described as remarkable, verifying that within the present set of assumptions the Knudsen layer correction to the stress is small (Hadjiconstantinou 2005). The

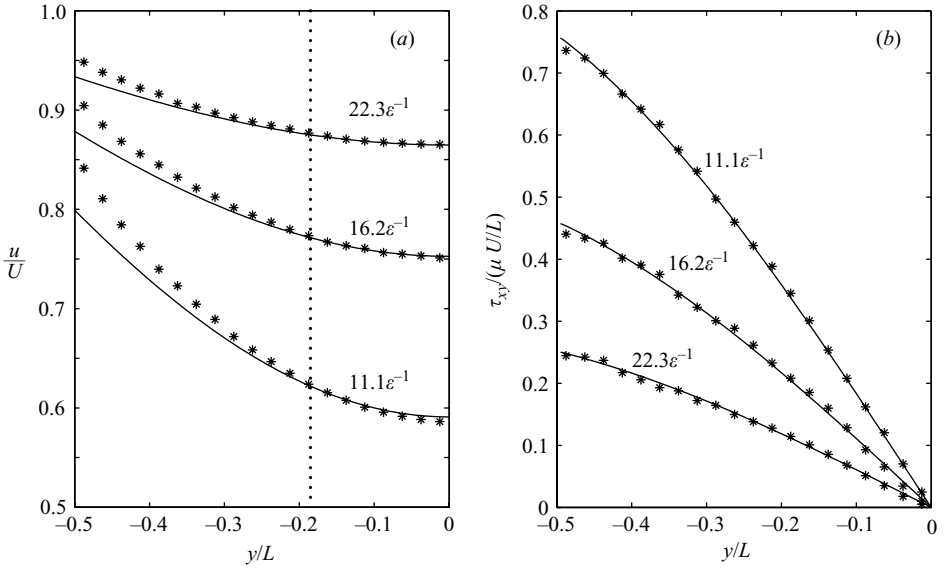

FIGURE 2. Comparison between DSMC results denoted by stars and the slip-corrected Navier–Stokes solution for $Kn = 0.21$ at three times. The wall is at $y/L = -0.5$. (*a*) A comparison of flow velocities (DSMC: u, Navier–Stokes: $\hat{u}$) and (*b*) a comparison of shear stress. The vertical dotted line in (*a*) delimits the extent of the Knudsen layer ($y/L \lesssim -0.185$).

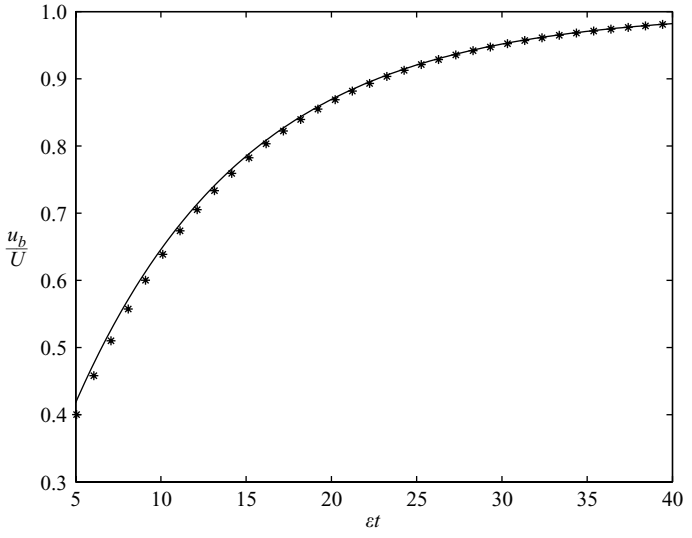

FIGURE 3. Comparison between DSMC results (stars) and the slip-corrected Navier–Stokes solution for $Kn = 0.21$ for the normalized average velocity (u_b/U) as a function of time.

average velocity obtained from equation (4.3), which corrects for the contribution of the Knudsen layer, is less than 1% different from the DSMC result (see figure 3).

4.3. *The timescale to steady state*

In this section we present results for the time taken for the bulk speed, u_b, to reach $0.9U$, denoted t_{90}. This timescale is useful because it gives information about the time taken to reach steady state and is related to the average force required to accelerate

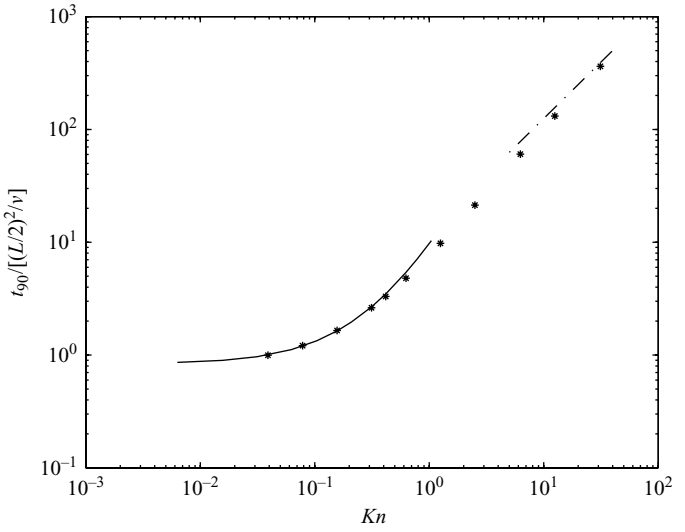

FIGURE 4. Normalized times t_{90} as a function of the Knudsen number. The solid line denotes the Navier–Stokes result subject to the second-order slip boundary condition (4.2) and the dash-dotted line denotes the collisionless result $t_{90}/[(L/2)^2/\nu] = 12.5Kn$. DSMC results are denoted by stars.

the gas. We normalize this time by $(L/2)^2/\nu = 8/(5\pi\varepsilon Kn^2)$, the momentum diffusion time for the Navier–Stokes problem. Figure 4 shows a comparison of the predicted t_{90} evolution timescales by the various models presented here as well as DSMC results. We observe the following: First, the models presented here have extended the description of this flow well into the transition regime. Second, the ballistic evolution timescale in the $Kn \gg 1$ limit is significantly longer than the diffusive-transport-based timescale. Finally, ballistic effects within the Knudsen layers result in a longer normalized evolution timescale. This effect is significant even at low Knudsen numbers, e.g. a factor of approximately 1.8 at $Kn = 0.2$. It is also perhaps remarkable that this effect, caused primarily by ballistic transport within the Knudsen layers, can be modelled by a purely diffusive mechanism, namely an effective increase in the physical domain length (equal to the sum of the two slip lengths).

5. Discussion

We have studied a transverse momentum transfer problem for arbitrary Knudsen numbers, and developed an analytical solution in the $Kn \gg 1$ limit to complement the Navier–Stokes result. We have also presented and evaluated a model that bridges the gap between the $Kn \ll 1$ and $Kn \gg 1$ limits. This work has led to a better understanding of the accuracy and limitations of second-order slip models and demonstrated that the slip model described in § 4.2 provides accurate descriptions of quantities of engineering interest, such as the stress and average flow velocity, at least up to $Kn \approx 0.4$.

The time evolution of the system is influenced by ballistic effects at surprizingly small Knudsen numbers. Even in the slip-flow regime where the overall flow field can be captured by the Navier–Stokes equations, the evolution timescale is found to be significanlty longer than the characteristic momentum diffusion timescale. Slip

models capture this increased timescale through the increased effective domain length implied by the slipping flow at the wall.

The primarily ballistic transport for $Kn \gg 1$ was studied by solving the linearized Boltzmann equation in the collisionless approximation. This solution was verified using DSMC simulations. Good agreement is found for $\varepsilon t \ll 1$ for all Kn both under early-time and late-time conditions.

The author is indebted to Professors Triantafyllos Akylas and Ioannis Kevrekidis for helpful comments and suggestions.

REFERENCES

Abramowitz, M. & Stegun, I. A. 1964 *Handbook of Mathematical Functions*. National Bureau of Standards, Applied Mathematics Series 55.

Alexander, F., Garcia, A. & Alder, B. 1998 Cell Size Dependence of Transport Coefficients in Stochastic Particle Algorithms. *Phys. Fluids* **10**, 1540–1542; and Erratum *Phys. Fluids* **12**, 731.

Cercignani, C. 1964 Higher order slip according to the linearized Boltzmann equation. *Institute of Engineering Research Rep.* AS-64-19. University of California, Berkeley.

Cercignani, C. 1988 *The Boltzmann Equation and its Applications*. Springer.

Garcia, A. & Wagner, W. 2000 Time step truncation error in direct simulation Monte Carlo. *Phys. Fluids* **12**, 2621–2633.

Hadjiconstantinou, N. G. 2000 Analysis of discretization in the direct simulation Monte Carlo. *Phys. Fluids* **12**, 2634–2638.

Hadjiconstantinou, N. G. 2003 Comment on Cercignani's second-order slip coefficient. *Phys. Fluids*, **15**, 2352–2354.

Hadjiconstantinou, N. G. 2005 Validation of a second-order slip model for dilute gas flows. *Microscale Thermophys. Enging* **9**(2) (to appear).

Ho, C. M. & Tai, Y. C. 1998 Micro-Electro-Mechanical Systems (MEMS) and fluid flows. *Annu. Rev. Fluid Mech.*, **30**, 579–612.

Maurer, J., Tabeling, P., Joseph, P. & Willaime, H. 2003 Second-order slip laws in microchannels for helium and nitrogen. *Phys. Fluids* **15**, 2613–2621.

Mills, A. F. 1992 *Heat Transfer*. Irwin.

Sone, Y. 1964 Kinetic theory analysis of linearized Rayleigh problem. *J. Phys. Soc. Japan* **19**, 1463–1473.

Wagner, W. 1992 A convergence proof for Bird's direct simulation Monte Carlo method for the Boltzmann equation. *J. Statist. Phys.* **66**, 1011–1044.